

Supplementary Information

Crossover in the dynamics of cell wall growth controls bacterial division times

S. Banerjee, K. Lo, T. Kuntz, M. Daddysman, A.R. Dinner and N.F. Scherer.

METHODS

Acquisition of experimental data. Data were acquired as in [1]. Briefly, the inducibly-sticky *Caulobacter crescentus* strain FC1428 was introduced into a microfluidic device and cells were incubated for one hour in the presence of the vanillate inducer. The device was placed inside a homemade acrylic microscope enclosure ($39'' \times 28'' \times 27''$) equilibrated to 31°C (temperature controller: CSC32J, Omega and heater fan: HGL419, Omega) and at other temperatures (see SI). At the start of the experiment, complex medium (peptone-yeast extract; PYE) was infused through the channel at a constant flow rate of $7 \mu\text{L}/\text{min}$ (PHD2000, Harvard Apparatus), which flushed out non-adherent cells. A microscope (Nikon Ti Eclipse with perfect focus system) and robotic XY stage (Prior Scientific ProScan III) under computerized control (LabView 8.6, National Instrument) were used to acquire phase-contrast images at a magnification of 250X (EMCCD, Andor iXon+ DU888 $1\text{k} \times 1\text{k}$ pixels; objective, Nikon Plan Fluor 100X oil objective plus 2.5X expander; lamp, Nikon C-HFGI) and a frame rate of 1 frame/min for 16 unique fields of view over 48 hours. In this manuscript we use a dataset consisting of 260 cells, corresponding to 9672 generations (division events) at 31°C .

Analysis of single cell shape. The acquired phase-contrast images were analyzed using a novel routine we developed (written in Python) [1, 2]. Each image was processed with a pixel-based edge detection algorithm that applied a local smoothing filter, followed by a bottom-hat operation. The boundary of each cell was identified by thresholding the filtered image. A smoothing B-spline was interpolated through the boundary pixels to construct each cell contour. Each identified cell was then tracked over time to build a full time-trajectory. We chose to include only cells that divided for more than 10 generations in the analysis. A minimal amount of filtering was applied to each growth curve to remove spurious points (e.g., resulting from cells coming together and touching, or cells twisting out of plane). The timing of every division was manually checked, so

the precision in determining this quantity results from the frame rate and not limitations of the automated analysis.

Cell wall growth assay. *C. crescentus* cells from the strain NA1000 were grown in 15 mL of M2X liquid culture media from 24 hours at 30°C to an optical density at 600 nm of 0.4. The swarmer cells from this liquid culture were isolated using a modified protocol by Marks and co-workers [3]. To summarize, the culture was spun at 6000 rpm for 20 minutes at 4°C. The pellet was then resuspended in 1 mL of cold M2 media. The culture was then spun at 13000 rpm for 3 min at 4°C. The pellet was then resuspended in 900 μ L of cold M2 media and 900 μ L of Percoll. The culture was then spun at 11500 rpm for 20 min at 4°C, yielding two bands of cells. The upper band consisting of stalked cells was aspirated off, leaving the lower band of swarmer cells. The swarmer cells were then washed twice with 1 mL of M2 and spun at 11000 rpm for 3 min. The pellet was resuspended in 5 mL of M2X and 100 μ L at a concentration of 1 mg/mL of fluorescent wheat germ agglutinin (fWGA), which had previously been shown to label the periphery of Gram-negative *E. coli* [4], was added to the resuspended culture and allowed to incubate with the cells for 10 min at 30°C to fully cover the cell wall. The culture was then diluted with 5 mL of M2X and grown in 30°C. 1 mL samples at 0, 20, 40, 60, 80, and 100 min were taken from the culture and frozen in dry ice. The cells were then fixed using 100 μ L paraformaldehyde and washed with 100 μ L phosphate buffered saline (PBS) and spun at 14000 rpm for 15 min. Microscope slides of the samples were made by combining 2 μ L of sample, 2 μ L of alginate, and 1 μ L of 0.3 M Ca^{2+} to immobilize the cells. Fluorescence images of the cells in the slides were obtained through confocal fluorescence microscopy (Supplementary Fig. 8A). The fluorescence data was obtained by using ImageJ by creating midline profiles of the cells and integrating the fluorescence intensity along the midline (Supplementary Fig. 8B). Deconvolution of fluorescence images (Fig. 2B) was performed using the Classic Maximum Likelihood Estimation algorithm of the Huygens Software (Scientific Volume Imaging). Parameters for the deconvolution were obtained from the measured point spread function of the confocal microscope (Nikon; Yokogama; 100x 1.45NA APO oil).

Growth uniformity index. A typical intensity profile at early times ($t < 40$ min) is spatially uniform around the cell center and then decays towards the poles. At later times, $t > 40$ min, the intensity profile is characterized by one minimum at the septum, given by I_{\min} , and two maxima at the stalked and the swarmer components, given by $I_{\max,1}$ and $I_{\max,2}$ respectively (Fig. 2D). At each time point, we define the growth uniformity index for each intensity pro-

file as, $D = 2I_{\min}/(I_{\max,1} + I_{\max,2})$. I_{\min} is defined as the minimum in the intensity profile for $r - 2\sigma < x/l < r + 2\sigma$, where x is the coordinate along the centerline, r is the mean ratio of the daughter cell lengths, and σ is the standard deviation in daughter cell length ratio. Let x_{\min} denote the location of I_{\min} along the centerline coordinate. Then $I_{\max,1}$ is defined as the maximum in the intensity for $x < x_{\min}$ and $I_{\max,2}$ is the maximum in the intensity profile for $x > x_{\min}$. Thus, for $t \leq 40$, $I_{\min} \simeq I_{\max,1} \simeq I_{\max,2}$ and $D \simeq 1$. Whereas for $t \geq 60$ min, I_{\min} represents the fWGA intensity value at the septum and is lower than both $I_{\max,1}$ and $I_{\max,2}$.

Size control models. The mixer model for size control (for $0 < t < \tau$) is defined by the following linear relationship between the size at birth, $l(0)$, and the size at division, $l(\tau)$,

$$l(\tau) = al(0) + \delta. \quad (\text{S.1})$$

where τ is the division time. From this model, a sizer, a timer or an adder model can be recovered by considering appropriate limits for the slope and the intercept. A sizer is defined by $a = 0$, whereas an adder assumes a slope of unity, $a = 1$. In the timer limit we have $\delta = 0$.

From the plot of $l(\tau)$ vs $l(0)$ (Fig. 1B), we determine the parameters a and δ by a least-square linear fit to the scatter. For an adder model fit, we constrain the slope to unity and determine the added size, δ , from the intercept. Similarly, for the timer model fit, we determine the slope by assuming a zero intercept, as was done in Ref. [1]. To determine which of these models more accurately represent our data, we evaluate the deviation of the models from the mean trend in our data. In particular we evaluate the following quantities:

$$\Delta_{\text{mixer}} = [al(0) + \delta] - \langle l(\tau) \rangle,$$

$$\Delta_{\text{adder}} = [l(0) + \delta] - \langle l(\tau) \rangle,$$

$$\Delta_{\text{timer}} = [al(0)] - \langle l(\tau) \rangle,$$

where the angular brackets mean ensemble average. As shown in Supplementary Figure 1A, $|\Delta_{\text{mixer}}| < |\Delta_{\text{adder}}| < |\Delta_{\text{timer}}|$. For initial cell sizes close to the ensemble mean $\langle l(0) \rangle$, all the models converge to $\langle l(\tau) \rangle$.

From the best fit parameters, a and δ , we can predict the relationship between the added size and the initial size,

$$\Delta l = (a - 1)l(0) + \delta,$$

and also between $\kappa\tau$ and $l(0)$

$$\kappa\tau = \ln \left(a + \frac{\delta}{l(0)} \right),$$

without requiring any additional fitting parameters. (Fig. 1C,E). The corresponding deviations in Δl and $\kappa\tau$ from their mean values are given in Supplementary Figures 1 B,C.

Prior to the onset of constriction ($0 < t < t_c$), we use a pure timer model for size control, as evidenced by our data (Fig. 3). This is given by,

$$l(t_c) = a'l(0), \quad (\text{S.2})$$

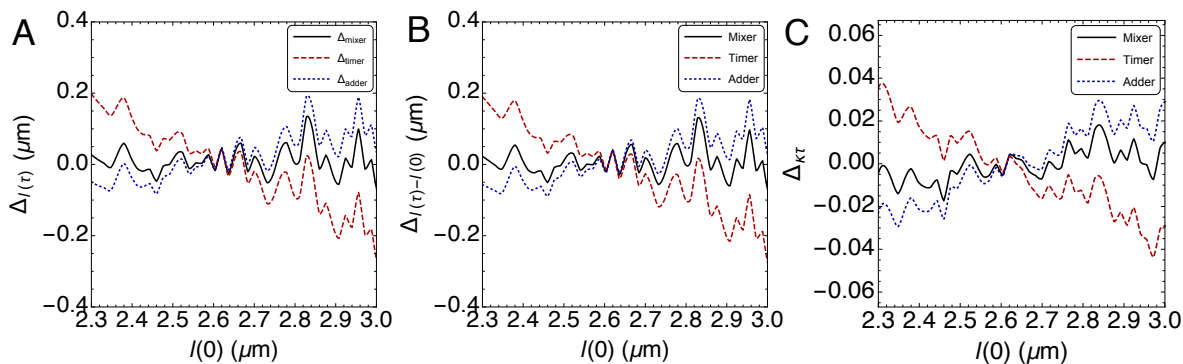
where a' is determined by fitting a line of zero intercept to the scatter plot of $l(t_c)$ vs $l(0)$. As a result, κt_c is constant and has a value $\simeq \ln(a')$.

During cell-wall constriction phase ($t_c < t < \tau$), we use a pure adder model for size control, as evidenced by our data (Fig. 3). This is given by,

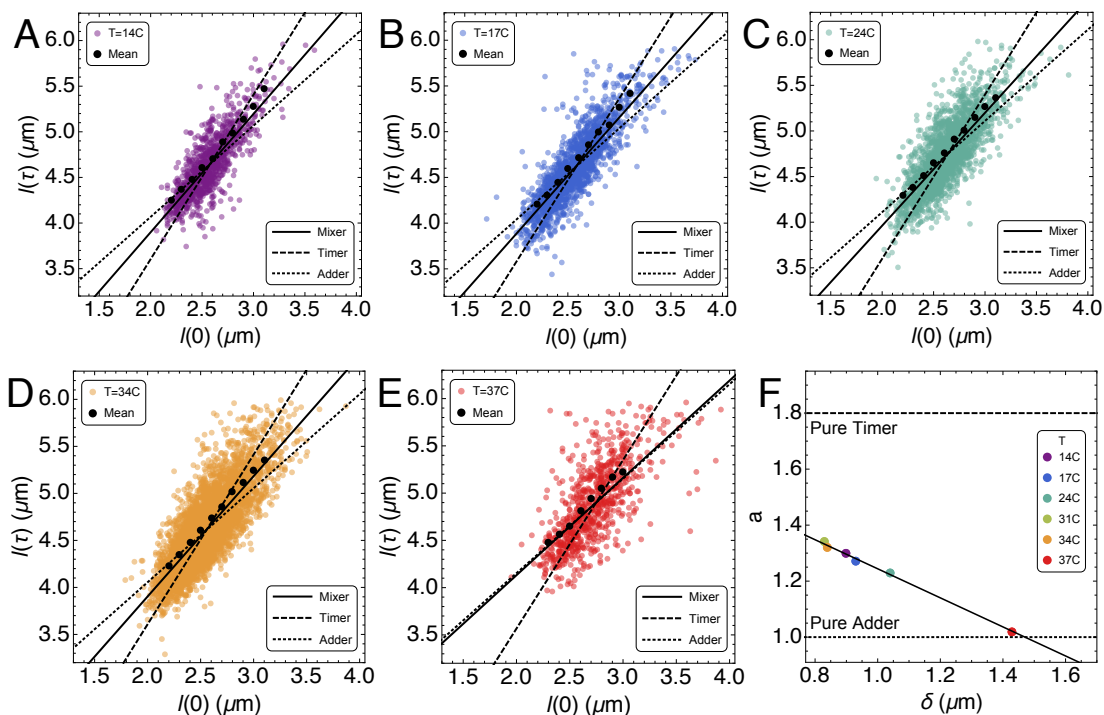
$$l(\tau) = l(t_c) + \delta', \quad (\text{S.3})$$

where δ' is determined by fitting a straight line of unit slope to the scatter plot of $l(\tau)$ vs $l(t_c)$. As a result, $\kappa(\tau - t_c)$ is negatively correlated with a value $\simeq \ln(1 + \delta'/l(t_c))$.

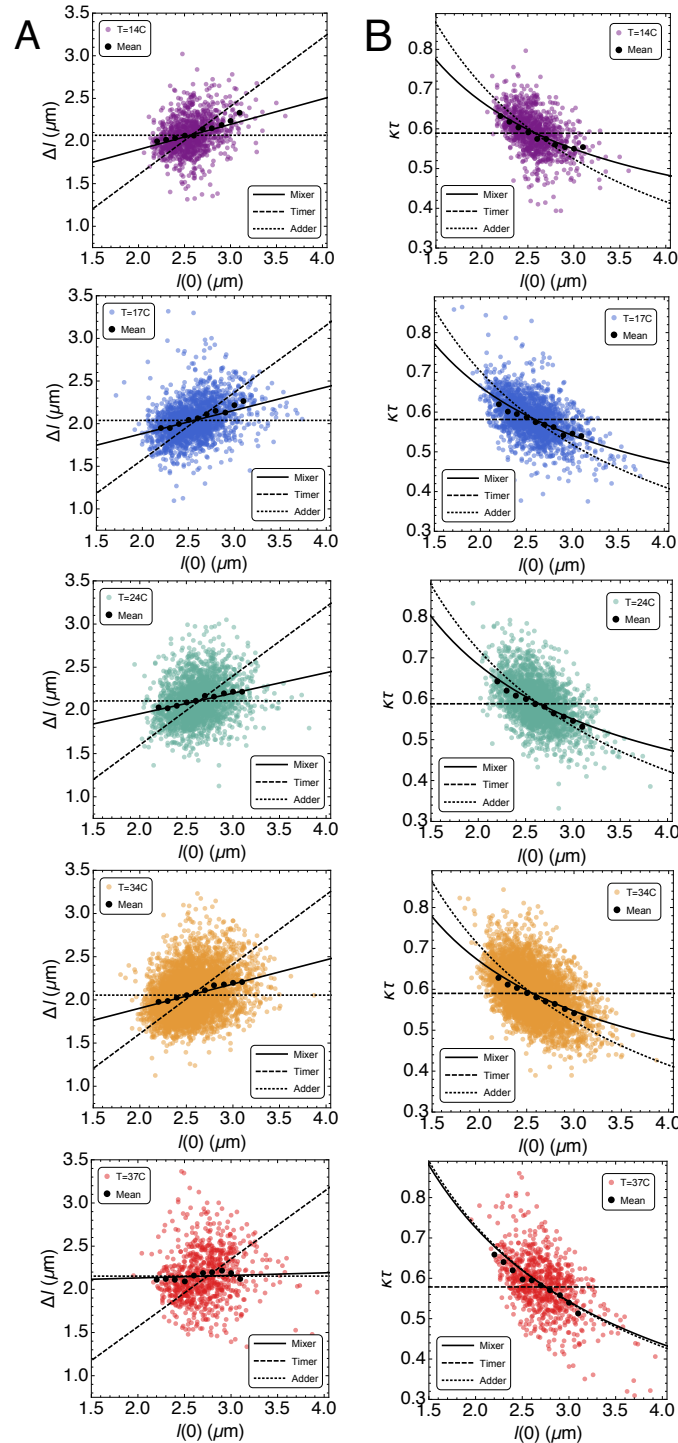
-
- [1] S. Iyer-Biswas, C. S. Wright, J. T. Henry, K. Lo, S. Burov, Y. Lin, G. E. Crooks, S. Crosson, A. R. Dinner, and N. F. Scherer, *Proceedings of the National Academy of Sciences* **111**, 15912 (2014).
 - [2] C. S. Wright, S. Banerjee, S. Iyer-Biswas, S. Crosson, A. R. Dinner, and N. F. Scherer, *Scientific Reports* **5**, 9155 (2015).
 - [3] M. E. Marks, C. M. Castro-Rojas, C. Teiling, L. Du, V. Kapatral, T. L. Walunas, and S. Crosson, *Journal of Bacteriology* **192**, 3678 (2010).
 - [4] T. S. Ursell, J. Nguyen, R. D. Monds, A. Colavin, G. Billings, N. Ouzounov, Z. Gitai, J. W. Shaevitz, and K. C. Huang, *Proceedings of the National Academy of Sciences* **111**, E1025 (2014).



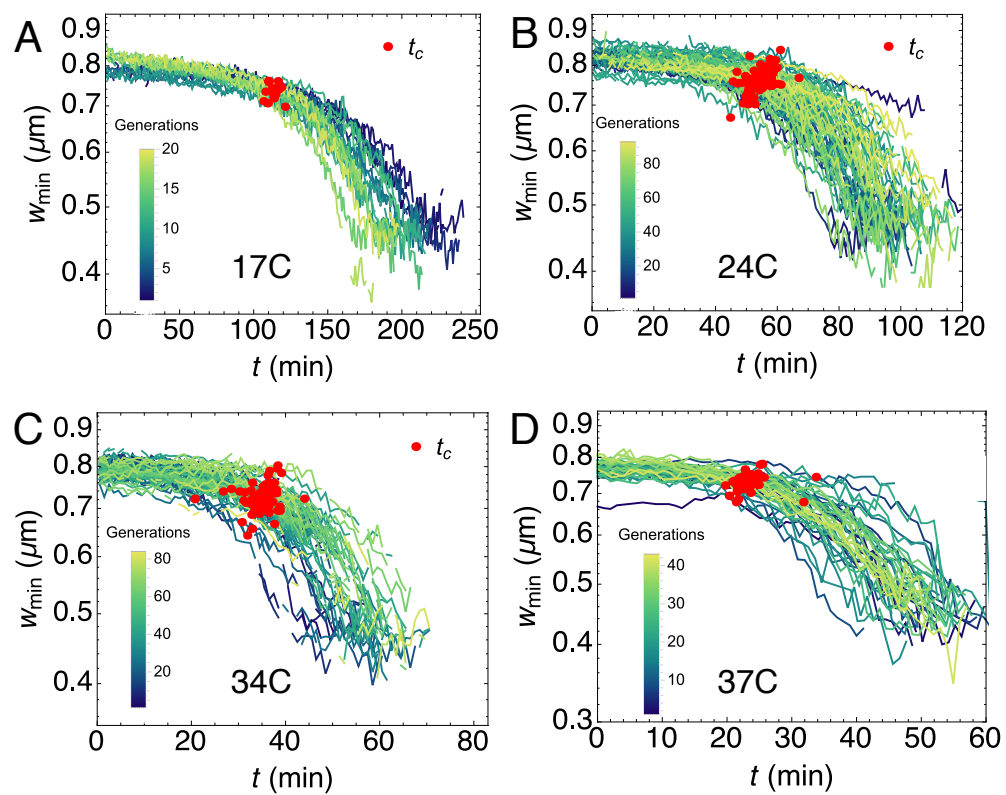
Supplementary Figure 1. Errors in size control models. Deviation about the mean for the (A) final length $l(\tau)$, (B) added length, $l(\tau) - l(0)$ and the (C) normalized cell cycle time, $\kappa\tau$, as given by a mixer (solid curve), adder (dotted curve) and a timer model (dashed curve).



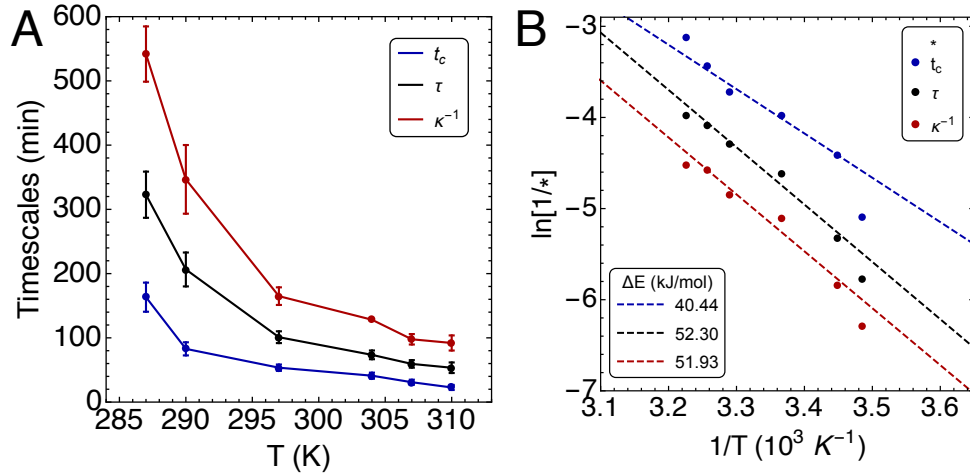
Supplementary Figure 2. Cell size regulation at various temperatures. (A-E) Correlation between the cell size at division, $l(\tau)$, and the cell size at birth, $l(0)$, at various temperatures. Black solid line represents a least square linear fit to the data (mixer model). Corresponding fits by timer and adder models are given by dashed and dotted lines, respectively. The solid circles represent mean data binned in $l(0)$. (F) Slope (a) and intercept (δ) of the mixer model as a function of temperature. With increasing temperature, cells approach the adder model of size control with $a \rightarrow 1$. Solid line is a least square linear fit, $a = -0.5\delta + 1.73$.



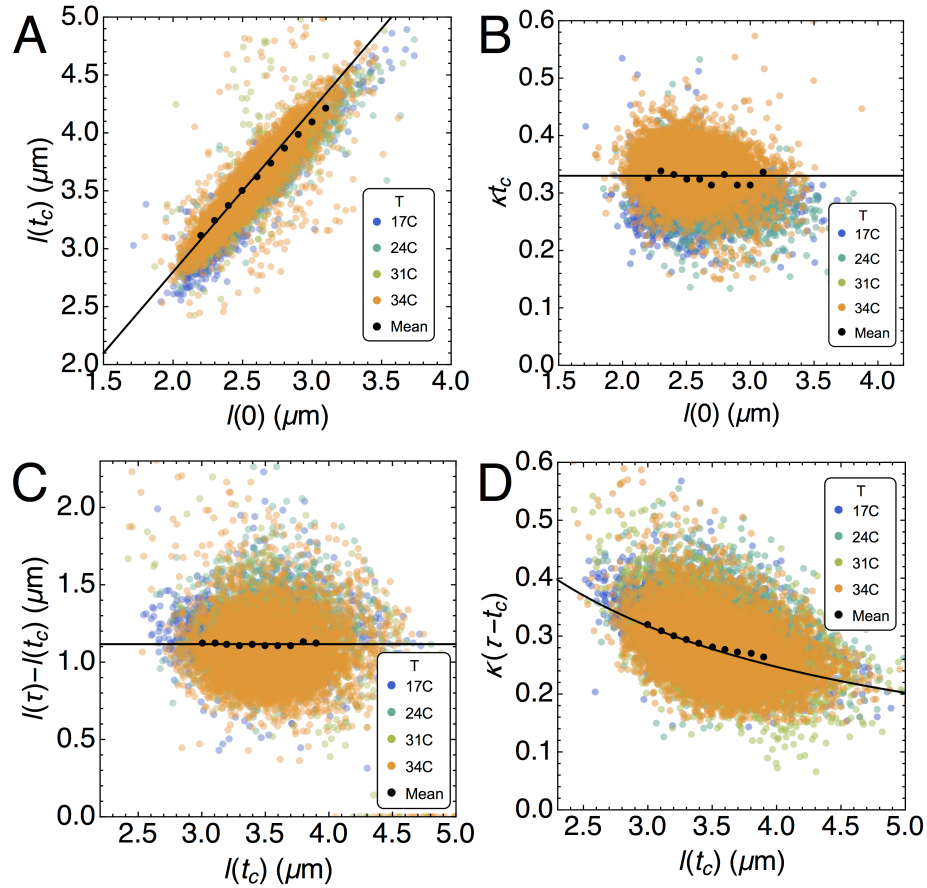
Supplementary Figure 3. Control of added size and division times at various temperatures. (A) Correlation between the added size, $\Delta l = l(\tau) - l(0)$, and the cell size at birth, $l(0)$, at various temperatures. (B) (Negative) Correlation between the normalized cell cycle duration, $\kappa\tau$, and the cell size at birth, $l(0)$, at various temperatures. Black solid line represents a least square linear fit to the corresponding data in Supplementary Fig. 1 (mixer model). Corresponding fits by timer and adder models are given by dashed and dotted lines, respectively. The solid circles represent mean data binned in $l(0)$.



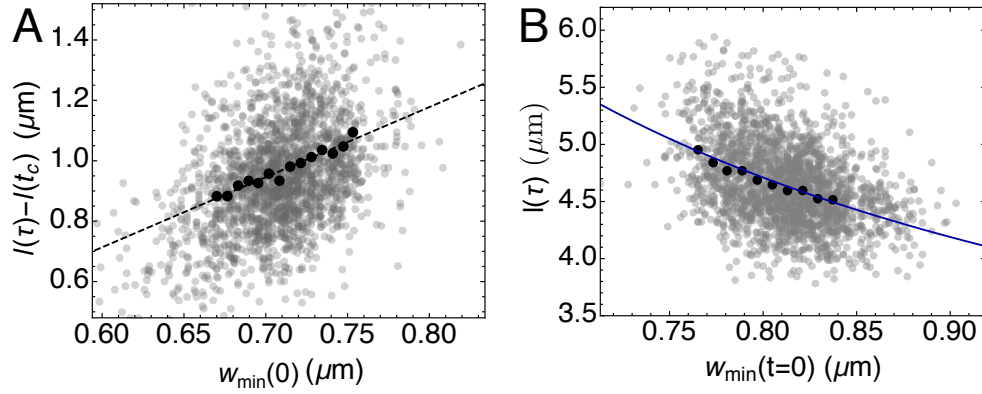
Supplementary Figure 4. Crossover dynamics at various temperatures. Dynamics of constriction ($w_{\min}(t)$) for a representative cell across all generations at temperatures: (A) 17C (B) 24C (C) 34C and (D) 37C.



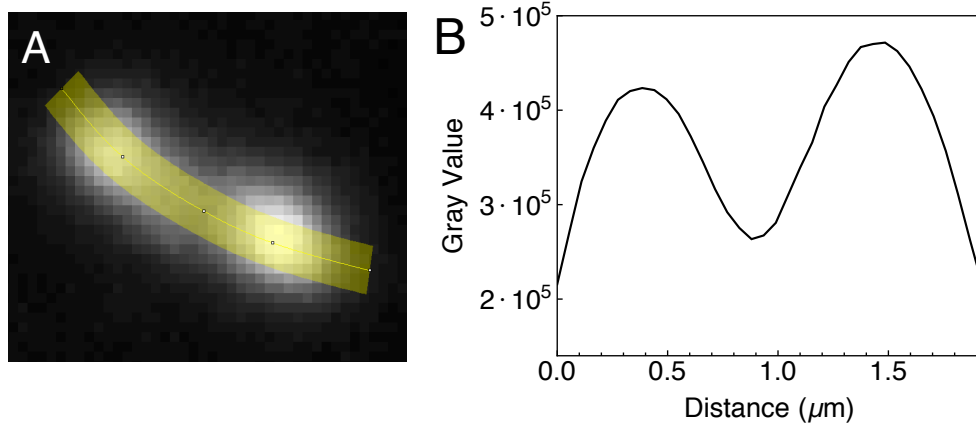
Supplementary Figure 5. Temperature variations of the crossover time. (A) The timescales t_c , τ and κ^{-1} monotonically decrease with increasing temperature. (B) Arrhenius plot for the variations of t_c , τ and κ^{-1} with temperature. We estimate the effective activation energy for crossing t_c to be $\Delta E \simeq 40$ kJ/mol, which is of the same order but less than the activation barrier for τ and κ^{-1} , $\Delta E \simeq 52$ kJ/mol. The estimate for ΔE comes from the slope of the dashed lines that are given by the Arrhenius equation: $\theta = \theta_0 e^{-\Delta E/k_B T}$, where θ represents κ , τ^{-1} and t_c^{-1} . We fit the Arrhenius equation in the temperature range 17°C-34°C. At lower (14°C) and higher (37°C) temperatures we observe a significant deviation from Arrhenius behavior, as discussed in [1].



Supplementary Figure 6. Timer to adder crossover at the onset of constriction at different temperatures. (A) Positive correlation between $l(t_c)$ and $l(0)$ is satisfied by a pure timer model, $l(t_c) = 1.4l(0)$. (B) Normalized crossover time, κt_c , is uncorrelated with cell size at birth with a mean value $\langle \kappa t_c \rangle = 0.33$ (C) Added size after constriction is uncorrelated with $l(t_c)$ at all temperatures, thus supporting a pure adder phase during constriction. Mean added size is $1.12 \mu\text{m}$. (D) Negative correlation between the normalized duration of constriction, $\kappa(\tau - t_c)$, and $l(t_c)$, consistent with a pure adder model. Solid curves in (A) and (B) are pure timer fits whereas in (C) and (D) they are pure adder fits.



Supplementary Figure 7. Cell shape controls cell size. (A) Correlation between $l(\tau) - l(t_c)$ and the septal width $w_{\min}(t_c)$. The solid circles represent mean data binned in $w_{\min}(t_c)$ and the dashed line is a linear fit to the scatter. (B) Negative correlation between final cell size, $l(\tau)$, and the initial septal width, $w_{\min}(0)$. The binned data are in solid circles; whereas the prediction of the septal growth model, $l(\tau) = \delta \left(1 - \frac{a}{1 + \Delta w_{\min}/l_0}\right)^{-1}$, is given by the solid line.



Supplementary Figure 8. Cell wall growth assay. (A) Fluorescence images of the cells obtained through confocal fluorescence microscopy and the construction of the midline axis (yellow bar). (B) The fluorescence data was obtained through ImageJ by creating midline profiles of the cells and integrating the fluorescence intensity along the midline.